Research Square

Preprints are preliminary reports that have not undergone peer review.
They should not be considered conclusive, used to inform clinical practice,
or referenced by the media as validated information.

Anlotinib Induced Venetoclax-resistant Acute Myeloid Leukemia Stem Cells Apoptosis through Downregulating Mcl-1-mediated Anti-apoptoeic Pathway

Bing Xu

xubing@xmu.edu.cn

Department of Hematology, The First Affiliated Hospital of Xiamen University and Institute of Hematology, School of Medicine, Xiamen University, Xiamen https://orcid.org/0000-0003-4273-5462

Qian Lai

The First Affiliated Hospital of Xiamen University and Institute of Hematology, School of Medicine, Xiamen University,

Yuchen Li

The First Affiliated Hospital of Xiamen University and Institute of Hematology, School of Medicine, Xiamen University,

Bowen Hou

The First Affiliated Hospital of Xiamen University and Institute of Hematology, School of Medicine, Xiamen University,

Jingwei Yao

Department of Hematology, The First Affiliated Hospital of Xiamen University and Institute of Hematology, School of Medicine, Xiamen University, Xiamen

Yuelong Jiang

The First Affiliated Hospital of Xiamen University and Institute of Hematology, School of Medicine, Xiamen University,

Jie Zha

The First Affiliated Hospital of Xiamen University and Institute of Hematology https://orcid.org/0000-0001-9376-3450

Article

Keywords: Acute myeloid leukemia (AML), Leukemia stem cells (LSCs), Venetoclax, Anlotinib, Mcl-1

Posted Date: December 1st, 2025

DOI: https://doi.org/10.21203/rs.3.rs-7977627/v1

License: This work is licensed under a Creative Commons Attribution 4.0 International License.
Read Full License

Additional Declarations: (Not answered)

Abstract

Acute myeloid leukemia (AML) is characterized by uncontrolled proliferation of leukemia stem cells (LSCs), which drive relapse and therapeutic resistance through mechanisms such as Mcl-1–mediated apoptosis evasion. Venetoclax, a selective Bcl-2 inhibitor, induces apoptosis in LSCs but is limited by acquired resistance. Anlotinib, a multi-target tyrosine kinase inhibitor, has demonstrated potential to overcome resistance by disrupting prosurvival signaling. This study investigated the synergistic antileukemic effects of Anlotinib and Venetoclax in overcoming Mcl-1–mediated resistance in AML LSCs. AML cell lines (Kasumi-1 and KG-1α) and primary $CD34^+CD38^-$ LSCs from patients (n = 31) were treated with Anlotinib, Venetoclax, or both. Cell viability and apoptosis were measured by CCK-8 and Annexin V/PI assays, while transcriptome sequencing and Western blot analyses elucidated the underlying molecular mechanisms. The combination therapy significantly enhanced apoptosis and inhibited proliferation in Venetoclax-resistant AML cells and LSCs compared with monotherapies. Mechanistically, Anlotinib potentiated Venetoclax by downregulating VEGFR2 and suppressing the PI3K/AKT/mTOR pathway, while the combination further inhibited the VEGFR2/SOS1/p38 axis, leading to decreased Mcl-1 expression. Immunoprecipitation confirmed that SOS1 promoted p-p38 accumulation, which was blocked by combination treatment. In NCG mice engrafted with primary AML cells, co-administration of Anlotinib and Venetoclax markedly reduced tumor burden and decreased p-p38 and p-AKT levels in xenograft tissues. These findings indicate that Anlotinib enhances Venetoclax sensitivity by targeting VEGFR2-dependent signaling and overcoming Mcl-1–mediated resistance, providing a promising therapeutic strategy for refractory AML.

Background

Acute myeloid leukemia (AML) is an aggressive clonal disorder of hematopoietic stem and progenitor cells, characterized by uncontrolled expansion of immature myeloid precursors[1, 2]. These immature cells accumulate in the bone marrow microenvironment, impairing hematopoiesis and leading to cytopenia through suppression of normal blood cell development[3]. At the apex of AML's cellular hierarchy are leukemia stem cells (LSCs), a therapeutically resistant population with dual capacities for self-renewal and clonal propagation. These relapse-initiating cells act as reservoirs for genetically distinct subclones, orchestrating epigenetically regulated differentiation cascades that drive disease heterogeneity[4]. Extensive evidence has established LSCs as central mediators of AML leukemogenesis, therapeutic resistance, and relapse[5]. The intrinsic resistance and adaptive plasticity of LSCs pose major clinical challenges, frequently resulting in treatment failure despite modern therapies[4, 6]. The molecular basis of LSC refractoriness involves multiple interconnected mechanisms: dormancy properties, niche-dependent interactions within hematopoietic tissues, and upregulation of pro-survival factors that circumvent chemotherapy-induced apoptosis[7]. The BCL-2 protein family, comprising central regulators of programmed cell death, critically modulates survival pathways in AML. These anti-apoptotic proteins sustain LSC viability through intricate apoptotic control, and their expression in LSCs predicts response to azacitidine/Venetoclax therapy[8]. Venetoclax has demonstrated clinical benefit by

inducing apoptosis in LSCs. Despite initial responses, however, Venetoclax efficacy is often limited by acquired resistance, leading to disease progression and reduced durability of clinical benefit in patients[9]. A recent study reported that Anlotinib synergized with Venetoclax in AML by inhibiting AML cells from entering mitosis[10]. Nevertheless, it remains unclear how Anlotinib modulates apoptosis regulation specifically in LSCs.

A clinical scoring system linking the ratio of BCL-2, BCL-xL, and MCL-1 protein expression in LSCs has been shown to predict AML treatment response[8]. MCL-1 is an essential anti-apoptotic protein in AML cells, and its expression is associated with poor prognosis and resistance to multiple chemotherapeutic agents [11].Studies demonstrate that MCL-1 confers resistance to BCL-2 inhibitors by substituting for BCL-2 and sequestering pro-apoptotic effectors, preventing their release to initiate cell death[12]. In addition, MCL-1 has been reported to directly activate mitochondrial oxidative phosphorylation in response to BCL-2 inhibition, thereby promoting metabolic homeostasis and LSC survival [13]. AML cells evade apoptosis by upregulating MCL-1 due to redundancy within the BCL-2 family, indicating that simultaneous targeting of multiple family members may be required to overcome resistance and achieve durable outcomes[13].

Anlotinib, a novel multi-target tyrosine kinase inhibitor (TKI), inhibits VEGFR, FGFR, PDGFR, and c-Kit and has emerged as a promising therapy for solid tumors[14, 15]. Its ability to disrupt signaling cascades involved in apoptosis regulation and angiogenesis suggests therapeutic potential for overcoming Venetoclax resistance in AML[16]. The rationale for combining Anlotinib with Venetoclax rests on the hypothesis that Anlotinib's broad mechanism of action may attenuate survival signals driving MCL-1 upregulation, thereby sensitizing AML cells to Venetoclax-induced apoptosis. This combination therapy may inhibit VEGFR2/SOS1/p38 signaling and directly downregulate MCL-1 expression, thus overcoming the limitations of monotherapy and providing a novel therapeutic strategy for refractory AML .

Our research aims to delineate the apoptotic regulatory mechanisms of this combination regimen in AML -LSCs, with particular focus on overcoming MCL-1–mediated resistance. Based on our data, Anlotinib and Venetoclax demonstrate complementary mechanisms: Anlotinib's broad kinase inhibition disrupts the cellular environment sustaining MCL-1's survival advantage, while Venetoclax selectively blocks BCL-2, creating a synergistic disruption of survival signaling in AML cells. This combination strategy could dismantle survival networks in AML -LSCs, providing a potent therapeutic avenue to address drug resistance.

Methods

This study aimed to investigate the apoptotic regulatory mechanisms of the combination of Anlotinib and Venetoclax in acute myeloid leukemia (AML) leukemia stem cells (LSCs), with a specific focus on overcoming MCL-1–mediated resistance. The study was designed as an experimental preclinical investigation using *in vitro* AML-LSC models to evaluate the synergistic effects of Anlotinib and

Venetoclax on survival signaling and apoptosis regulation. All experiments were conducted in a laboratory setting under standardized culture conditions to ensure reproducibility and accuracy of results.

Cell line culture

The AML cell lines (Kasumi-1 and KG-1α) were maintained in our laboratory. AML cell lines were cultured in RPMI 1640 medium (PM150110, Procell, China) supplemented with 10% or 20% fetal bovine serum (FBS), 10 mM L-glutamine, 100 U/ml penicillin, and 10 mg/ml streptomycin (HyClone™, Logan, UT, USA). Cells were incubated at 37°C in a humidified atmosphere containing 5% CO_2. KG-1α cells were cultured in IMDM(PM150510, Procell, China) supplemented with 100 U/ml penicillin, 100 μg/ml streptomycin (1 × P/S), and 10% FBS (FBS) (HyClone TM, Logan, UT, USA).

Patients and donor samples

Primary bone marrow samples from patients with AML (n = 31) were obtained from the Department of Hematology, First Affiliated Hospital of Xiamen University. This study was conducted in accordance with the Declaration of Helsinki and was approved by the Ethics Review Board of the First Affiliated Hospital of Xiamen University. Clinical characteristics of patients with AML are summarized in Table 1. Mononuclear cells were isolated by density gradient centrifugation using Ficoll (BD, Franklin Lakes, NJ, USA) and cultured briefly in RPMI 1640 supplemented with 10% FBS.

Drug screening

Cell cytotoxicity and viability were assessed using the CCK-8 assay. A library of 4,414 compounds (Cat: L9200, TargetMol) at a concentration of 10 μM was screened against KG-1α cells using the PerkinElmer high-throughput screening system (Waltham, MA, USA), with DMSO serving as the control. Cells were seeded into 384-well plates and incubated for 24 h. Subsequently, 5 μL of CCK-8 reagent was added to each well, and after an additional 1–2 h of incubation, cell viability was measured using Varioskan Flash (Thermo Scientific).

Cell viability assay

Cell proliferation was measured using a CCK-8 kit (MCE, Shanghai, China). Cells (3×10^4 cells/well) were plated in 96-well plates with 100 μL growth medium and treated with Anlotinib and Venetoclax at designated doses for 48 h and 72 h. Following treatment, CCK-8 reagent was added and incubated for 1–4 h, and absorbance at 450 nm was detected by Varioskan Flash (Thermo Scientific). All experiments were performed three times in triplicate.

Drug-dose-response experiments and CalcuSyn analysis

For Anlotinib–Venetoclax combination experiments, compounds were added simultaneously and relative cell number was determined at 48 h. Synergy was analyzed by calculating combination index values using CalcuSyn Version 2.1 software.

Flow cytometry detection of apoptosis

Apoptosis of non-LSC-like or LSC-like cells was evaluated by flow cytometry after Annexin V and PI staining (FXP018-100, 4A Biotech) according to the manufacturer's instructions. In brief, cells exposed to different treatments were harvested, washed with ice-cold PBS (Gibco, USA) and 1 × Annexin V binding buffer, and then subjected to Annexin V-FITC/PI staining. Flow cytometric analysis was performed within 1 h after staining. Primary samples exhibiting spontaneous apoptosis greater than 30% without treatment were excluded and stained with human CD34-APC antibody (clone 581, BioLegend) and human CD38-PE antibody (clone HB-7, BioLegend, USA) to determine stemness characteristics.

Cell cycle analysis by EdU incorporation assay

The cell cycle was analyzed using an EdU Cell Proliferation Kit(Cat:C0081L, Beyotime, China), following the manufacturer's guidelines, with the process incorporating an EdU assay. In brief, cultured cells were treated with EdU at a final concentration of 20 μM and incubated for 1 h. After incubation, the cells were harvested and rinsed with PBS. The cells were then fixed and permeabilized with 50 μL Fixation/Permeabilization buffer (composed of Fixation/Permeabilization Concentrate and Diluent) for 30 min at room temperature, followed by a rinse with 1× permeabilization buffer. The pellet was resuspended in the Click additive solution and incubated for 30 min. After the Click reaction, cells were rinsed twice. Finally, DAPI was added before flow cytometry, and data were analyzed using FlowJo software.

JC-1 Mitochondrial Membrane Potential

Collect 1 × 10^5 cells/well and resuspend in 0.5 ml cell culture medium. Add 0.5 ml JC-1 staining working solution(C2006, Beyotime Biotechnology, China) and invert several times to mix. Incubate at 37°C in a cell culture incubator for 20 min. During incubation, prepare JC-1 staining buffer (1×) by diluting with distilled water at a ratio of 4 ml per 1 ml of JC-1 staining buffer (5×) and place on ice. After incubation, centrifuge at 600 g at 4°C for 3–4 min to pellet cells. Discard the supernatant carefully. Wash twice with JC-1 staining buffer (1×): add 1 ml, resuspend, centrifuge at 500 g at 4°C for 3–4 minutes, and discard the supernatant. Repeat once more. Finally, resuspend in JC-1 staining buffer (1×) and analyze by flow cytometry.

Transcriptome sequencing

Total RNA from Kasumi-1 cells was sequenced at BGI-Shenzhen using the Illumina HiSeq 2000 platform. Raw sequencing reads containing adaptors, more than 10% unknown bases, or more than 50% low-quality bases per read were filtered out. Gene expression levels were reported as reads per exon kilobase per million.

Western blot analysis

Cells (2 × 10^5/well) were treated with Anlotinib, Venetoclax, or DMSO for 12 h. Apoptosis was measured to ensure rates remained below 10% before immunoblotting. Cells were lysed in RIPA buffer (P0013C,Beyotime Biotechnology, China) containing protease inhibitor cocktail (C0001, Topscience, China) and phosphatase inhibitor cocktail (C0004, Topscience, China). Protein concentrations were determined with a BCA Protein Assay (20200ES76, Yeasen, China). Samples were mixed with SDS loading buffer, boiled for 10 min, and loaded (20 μg/lane) onto SDS-PAGE gels for protein separation. Proteins were transferred to PVDF membranes (Millipore, UK), blocked with 5% non-fat milk, and incubated with primary antibodies, including anti-c-Kit(18691-1-AP, Proteintech, USA) and antibodies from Cell Signaling Technology (Danvers, MA, USA): anti-VEGFR2 (2479), anti-PDGFRα(3174), anti-FGFR1 (9740), anti-PI3K(4249), anti-PARP (9542), anti-p-p38 MAPK(Thr180/Tyr182) (4511), anti-p38 MAPK (9212), anti-Phospho-Stat5(4322S), anti-Bcl-2 (4223S), anti-Mcl-1 (4572), anti-p-Mcl-1 (Thr163) (14765), anti-SOS1 (5890), and anti-GAPDH(D16H11). Membranes were washed with TBST (Tris-buffered saline with Tween 20) to remove unbound antibody. After incubation with HRP-conjugated secondary antibodies, signals were detected using enhanced ECL substrate (GE Healthcare, Chicago, USA) and visualized with the Amersham Imager 600 (AI600, GE Healthcare, Chicago, USA).

Human AML xenograft experiments

All animal experiments were approved by the Animal Center of Xiamen University (Xiamen, China). Equal numbers(1×10^6)of $CD34^+$ primary AML cells were injected into NOD-*Prkdc*$^{-/-}$*IL2rg*$^{-/-}$tm1Bcg (NCG) mice (GemPharmatech Ltd., Beijing, China) after 1 Gy irradiation via tail vein. To confirm engraftment, peripheral blood was stained with human CD45 and mouse CD45 after ACK buffer lysis. Once the tumor burden exceeded 1%, mice were divided randomly into four groups. Anlotinib（Selleckchem Houston, TX) and Venetoclax（T2119, Topscience, China) were dissolved in DMSO and administered orally at 10 mg/kg for 14 consecutive days. At the study endpoint, NSG mice were sacrificed, and tumor burden was analyzed using human CD45-FITC (clone HI30, BioLegend), mouse CD45-BV421 (clone 30-F11, BD Horizon), and human CD34-APC (clone 581, BioLegend).

Immunoprecipitations

For SOS1 immunoprecipitation assays, Kasumi-1 and KG-1α cell pellets were harvested at 500 g for 5 min at 4°C. The supernatant was removed, and the pellet was resuspended in 1 mL PBS.Kasumi-1 and KG-1α cells were then lysed in ice-cold RIPA buffer (Beyotime, Shanghai, China) supplemented with protein phosphatase inhibitor (TargetMol Chemicals Inc., USA) and complete protease inhibitor cocktail (TargetMol Chemicals Inc., USA). Lysates were clarified by centrifugation at 14,000 g for 10 min. Pre-clearing was performed with Protein A/G agarose beads (Santa Cruz) for 45 min, and

immunoprecipitation was conducted for 2 h with SOS1 antibody or rabbit IgG. Protein complexes were captured with Protein A/G agarose beads overnight at 4°C on a vertical roller, washed three times in ice-cold RIPA buffer, and eluted by boiling in SDS sample buffer for Western blot analysis.

Statistical analysis

All statistical analysis for *in vitro* and *in vivo* studies was performed using GraphPad Prism Software (v5.0). Unpaired Student t tests were performed with $P < 0.05$ as the cutoff for statistical significance. All data are presented as mean ± SEM. *, $P < 0.05$; **, $P < 0.01$; ***, $P < 0.001$.

Results

Anlotinib is the potential combination choice for Venetoclax-resistant LSC

We first trained the Venetoclax-resistant LSC cell lines to identify the best combination strategies that enhance the pro-apoptotic effect of Venetoclax. Venetoclax-resistant LSC cell lines exhibited an increased proliferation rate upon Venetoclax treatment compared to sensitive LSC cell lines (Fig. 1A, B). Flow cytometry analysis using Annexin V/PI staining confirmed that Venetoclax induced significantly lower apoptosis in Kasumi-1-R and KG-1α-R cells compared with wild-type controls (Fig. 1C–F), confirming acquired resistance. To assess whether primary AML-LSCs also exhibit intrinsic resistance, primary $CD34^{+}CD38^{-}$ cells isolated from AML patients were subjected to Venetoclax treatment. Flow cytometry analysis revealed limited apoptotic response in primary LSCs (Fig. 1G, H), suggesting a broad Venetoclax resistance pattern across stem-like AML populations. A high-throughput drug screening system was hired to identify synergistic combinations of drug targets in Venetoclax-resistant LSCs. The results revealed that TKI inhibitor Anlotinib was one of the top-most active drugs based on the area over the lethal (Fig. 1I).

Fig 1:Anlotinib is the potential combination choice for Venetoclax-resistant LSC

(A, B) Cell viabilities in Venetoclax-resistant Kasumi-1-R and KG-1α-R cells for 24 hours.

(C, D) Quantification of apoptosis in leukemia stem-like cell lines Kasumi-1 wild type and Kasumi-1 Venetoclax-resistant cell lines after treatment with Venetoclax for 24 h.

(E, F) Flow cytometry plots depict the gating approach used to identify apoptotic cells in Kasumi-1 wild-type and Kasumi-1 Venetoclax-resistant cell lines by staining Annexin V(AV) and Propidium iodide(PI).

(G)Flow cytometry plots depict the gating approach used to identify the primary leukemia stem cell by stanning human CD34 and human CD38 and the apoptotic cells by stanning Annexin V(AV).

(H)Quantification of apoptosis in primary leukemia stem cell after treatment by Venetoclax for 24 h.

(I)High-throughput drug screening identifies Anlotinib as a synergistic compound with Venetoclax in targeting leukemia stem-like cells.

Anlotinib resensitizes the Venetoclax-resistant LSC cell by increasing cell apoptosis.

We next tested the potential combination of Anlotinib and Venetoclax in AML LSC-like cell lines (Kasumi-1 and KG-1α) according to recent LSC studies[17]. We first evaluated the inhibitory effect of Anlotinib and Venetoclax using the CCK-8 assay, which demonstrated that combined treatment suppressed cell proliferation more effectively than single agents in a dose-dependent manner in both cell lines (Fig. 2C, F). To examine the cell cycle regulatory effect of combining Anlotinib and Venetoclax on AML cells, as noted by other groups, DAPI and EdU staining were employed to assess cell cycle distribution. Combination therapy increased the proportion of cells in G0/G1 and reduced those in S-phase （Fig. S1A-D. A distinctive feature of early programmed cell death and cell cycle progression is mitochondrial disruption. We further investigated mechanisms of combination-induced apoptosis. JC-1 and γ-H2AX were detected by flow cytometry to evaluate mitochondrial potential and DNA damage. Combination therapy increased mitochondrial depolarization detected by JC-1（Fig 2K-L）, consistent with PARP-dependent apoptosis（Fig 2N. γ-H2AX, a DNA damage marker, recruits repair proteins to sites of damage and regulates both cell cycle and apoptosis. Our results showed that combined treatment induced DNA damage, confirmed by increased γ-H2AX staining (Fig S1E–F) and upregulation of p-H2AX (Fig S1H). These findings indicated that combination therapy inhibited LSCs by promoting apoptosis and inducing DNA damage.

Fig 2. Anlotinib resensitize the Venetoclax-resistant LSC cell through increasing cell apoptosis.

(A, D) Immunomarker of leukemia stem-like cells in Kasumi-1 and KG-1α cell lines by flow cytometry.

(B, E) Proliferation analysis of leukemia stem-like cell lines Kasumi-1 and KG-1α after treatment with combined candidate drugs and Venetoclax.

(C,F) Combination index (CI) in the indicated two cell line cells was analyzed by CalcuSyn software. CI > 1 indicates antagonist effect; CI = 1 indicates additive effect; CI < 1 indicates synergistic effect.

(G,I) Flow cytometry plots depict the gating approach used to identify apoptotic cells in Kasumi-1 and KG-1α cell lines by staining AV and PI.

(H,J) Quantification of apoptosis in leukemia stem-like cell lines Kasumi-1 and KG-1α. Bar graphs show the percentage of Annexin V-positive, PI-negative early apoptotic cells in Kasumi-1 and KG-1α cell lines, as determined by flow cytometry.

(K,M) Gating strategy for mitochondrial membrane potential analysis in leukemia stem-like cell lines Kasumi-1 and KG-1α using JC-1 staining.

(L) Quantification of mitochondrial membrane potential changes in leukemia stem-like cell lines Kasumi-1 and KG-1α using JC-1 staining.

(N) Western blot analysis of the apoptosis marker PARP in leukemia stem-like cell lines Kasumi-1 and KG-1α under different drug treatment for 12 hours.

Anlotinib enhances the effect of Venetoclax in inhibiting the VEGF/PI3K/AKT signaling pathway

To investigate the mechanism by which Anlotinib enhances Venetoclax-mediated cytotoxicity, we performed RNA sequencing on control cells, single-agent–treated cells, and combination-treated cells. Combination therapy showed distinct gene expression profiles compared with other groups (Fig. S2). KEGG enrichment analysis revealed that the PI3K/AKT pathway, VEGF pathway, and apoptosis-related pathways were significantly enriched in the combination group compared with Venetoclax alone (Fig 3A). Notably, these pathways were consistently enriched in the combination group (Fig. 3B, Fig. S2C-D). We then examined Anlotinib target proteins. VEGFR-2 was downregulated after combination treatment, whereas PDGFR, FGFR, and c-Kit were not (Fig 3C, D). GSEA enrichment analysis further revealed downregulation of CDK2, a cell cycle–associated protein (Fig S2D,E). We next evaluated cargo proteins regulated by VEGFR-2 and found that PI3K/AKT signaling was decreased. Reduced levels of PI3K, mTOR, and AKT were confirmed in both LSC lines (Fig 3E,F). These results confirmed that Anlotinib potentiates Venetoclax-induced apoptosis by inhibiting VEGF/PI3K/AKT signaling.

Fig 3. Anlotinib enhance the effect of Venetoclax in inhibiting the VEGF/PI3K/AKT signaling pathway

(A) KEGG enrichment analysis of differential expression genes detected by RNA-Seq of Kasumi-1 cell line comparing combination regimen and venetoclax-only regimen. GSEA enrichment analysis of differential expression genes detected by RNA-Seq of Kasumi-1 cell line comparing combination regimen and venetoclax-only regimen.

(C,D) The expression levels of the targets protein of Anlotinib in Kasumi-1,KG-1α cell lines.

(E,F)Expression and phosphorylation levels of PI3K/AKT signaling pathway in Kasumi-1, KG-1α cell lines after the treatment of combining Anlotinib and Venetoclax and alone.

Anlotinib reverses Venetoclax-induced overexpression of Mcl-1 by inhibiting SOS1.

We next examined apoptosis-related Mcl-1 expression in Venetoclax-resistant LSCs. As shown in the figure, Mcl-1 expression in AML-LSCs was higher than in sensitive LSCs Fig. 4A, B. To determine whether Anlotinib enhances the effect of Venetoclax by inhibiting Mcl-1, we assessed VEGFR-2 and its upstream regulatory protein Grb2. Immunoblotting demonstrated that the VEGFR/Grb2/SOS1 pathway and the p38/GSK/Mcl-1 pathway were inhibited by Anlotinib and Venetoclax combination treatment in both LSCs (Fig. 4E, F). We next investigated changes in SOS1–p-p38 interactions during Mcl-1 suppression by performing immunoprecipitation(IP). Immunoprecipitation showed that SOS1 accumulated p-p38 under combination therapy Fig. 4G, H. These findings indicated that decreasing SOS1 can overcome intrinsic

and acquired Bcl-2 inhibitor resistance through p38/GSK3/ Mcl-1 signaling by promoting Mcl-1 degradation.

Fig 4 Anlotinib reverses Venetoclax-induced overexpression of Mcl-1 by inhibiting SOS1.

(A,B) Western blot shows the original expression of Mcl-1 and Bcl-2 in Venetoclax-resistant Kasumi-1-R and KG-1α-R cells.

(C,D) Immunoblots showing the levels of indicated protein in Kasumi-1 and KG-1α cells after treatment with Anlotinib and Venetoclax alone and combination.

(E,F) The expression of p38/GSK3/ Mcl-1 pathway signaling in Kasumi-1 and KG-1α cells.

(G,H) SOS1 can accumulate p-p38 in response to the treatment of combination of the Anlotinib and Venetoclax.

SOS1 activation restores Venetoclax resistance in LSCs *in vitro*.

Immunoblotting revealed that SOS1 was overexpressed in AML-LSCs but not in non–AML-LSCs (Fig. 5A, B). To verify the regulatory role of SOS1 in LSCs treated with Anlotinib and Venetoclax, we overexpressed SOS1 in Kasumi-1 and KG-1α cells and observed augmented Mcl-1 expression (Fig. 5C, D). We then performed a CCK-8 assay to assess whether SOS1 overexpression in Kasumi-1 and KG-1α increased cell viability. As expected, cell viability was higher in SOS1-overexpressing cells compared with controls (Fig. 5E, F). Next, we tested the pro-apoptotic effect of combining Anlotinib and Venetoclax *in vivo.* Combined treatment significantly reduced spleen size and weight (Fig. 5G, H). Human $CD45^+$ cell ratios in spleen, peripheral blood, and bone marrow were decreased following combination therapy (Fig 5I-K). Taken together, SOS1 acts as a key regulator in Anlotinib-Venetoclax-induced LSC apoptosis.

Fig 5 SOS1 activation restores Venetoclax resistance in LSCs *in vitro*.

(A,B) Basic expression of SOS1 in KG-1α, Kasumi-1, MOLM-13, OCI-AML-2, OCI-AML-3,THP-1, and MV-4 11 cells.

(C,D) Immunoblotting of SOS1 and Mcl-1 in SOS1 overexpressed and wild type AML-LSCs cell lines.

(E,F) Cell viability test of the SOS1 overexpressed and wild type AML-LSCs cell lines.

(G) Representative spleen images of CDX models of gavage carrier, Alotinib, Venetoclax, or their combination.

(H) Quantitative analysis of spleen weight (n=4/group).

(I-K) Flow cytometry revealed the percentage of $hCD45^+$ leukemic cell proportion in spleen, peripheral blood and bone marrow for Kasumi CDX models.

(L) Schematic outline of the CDX model.

The combination of Anlotinib and Venetoclax reciprocally overcome the resistance of AML primary samples *in vitro* and *in vivo*.

Next, we performed flow cytometry analysis to assess the pro-apoptotic effect of combination treatment in primary AML samples. After exposure to the combination, apoptosis was measured using AnnexinV/PI co-staining. As expected, the combination of Anlotinib and Venetoclax effectively induced apoptosis in primary patient samples (Fig. 6A-D). Since leukemia stem cells possess the capacity for disease regeneration, we next examined whether the combination could inhibit LSC function. Primary patient leukemia cells enriched for $CD34^+$ were engrafted into sublethally irradiated immunodeficient mice. Combination therapy significantly prolonged PDX survival (Fig. 6E). To evaluate engraftment, PDX mice were sacrificed, revealing decreased human $CD45^+$ cell engraftment in peripheral blood and bone marrow with the combination treatment (Fig. 6G-I). Monotherapy with Anlotinib or Venetoclax slightly decreased or increased spleen weight and human $CD45^+$ engraftment, whereas the combination dramatically reduced both (Fig. 6J). Spleen size was also markedly reduced in combination-treated mice (Fig. 6F). These data confirmed that Anlotinib plus Venetoclax restored pro-apoptotic activity in primary AML samples.

Fig 6. The combination of Anlotinib and Venetoclax reciprocally overcome the resistance of AML primary samples *in vitro* and *in vivo*.

(A,B) Flow cytometry showing the gate strategy to determine $CD34^+$ AML LSC subpopulation.

(C) Apoptosis rates of $CD34^+$ primary AML sample induced by the combination of Anlotinib and Venetoclax for 12 hours.

(D) Cell viability test of $CD34^+$ primary AML sample upon the combination of Anlotinib and Venetoclax for 12 hours.

(E) The survival was monitored over time and the Kaplan-Meier survival curves of PDX (n=4/group) was shown. Statistical significance was evaluated the long rank test.

(F) Representative spleen images of PDX models of gavage carrier, Anlotinib, Venetoclax, or their combination.

(G-I) Flow cytometry analysis of hCD45 percentage in peripheral blood,bone marrow and spleen was shown.

(J)The spleen weight of mice in the four groups was assessed at the same time points after sacrificed.

(K) Representative HE staining of PDX mice bone marrow.

(L) Representative IHC staining of SOS1 in PDX mice liver.

Inhibition of p38 and AKT signaling by combination treatment in PDX models.

To further verify the mechanism by which combination therapy overcomes Venetoclax resistance *in vivo*, we performed immunohistochemical (IHC) analysis of p38 and AKT in the spleen, liver, and kidney of PDX mice. Spleen tissues from the combination group exhibited markedly reduced levels of phosphorylated p38 (p-p38) and phosphorylated AKT (p-AKT) compared with control and monotherapy groups (Figure 7A). Quantitative analysis confirmed significant downregulation of both p-p38 and p-AKT in the spleen, while total p38 and AKT levels remained relatively unchanged (Figure 7B). Similar trends were observed in the liver (Figure 7C), where combination therapy significantly suppressed p-p38 and p-AKT expression (Figure 7D), suggesting systemic inhibition of stress and survival signaling. In the kidney (Figure 7E), reductions in p-p38 and p-AKT levels were also evident, though slightly less pronounced than in spleen and liver tissues. These results indicate that Anlotinib and Venetoclax effectively suppress p38 and AKT pathway activation *in vivo*. H&E staining revealed notable histological restoration in the spleen and kidney of the combination group, suggesting a protective effect at the tissue level (Figure 7G). Western blot analysis further validated the IHC findings, showing decreased phosphorylation of p38 and AKT in spleen lysates from combination-treated mice (Figure 7H).

Fig 7 : Inhibition of p38 and AKT signaling by combination treatment in PDX models.

(A, C, E) Representative IHC staining images of spleen (A), liver (F), and kidney (K) tissues from PDX mice treated with vehicle (Control), Anlotinib, Venetoclax, or the combination (Comb). Sections were stained for total p38, phosphorylated p38 (p-p38), total AKT, and phosphorylated AKT (p-AKT). Scale bar = 30 μm.

(B) Quantification of IHC staining intensity in spleen tissues for p38, p-p38 AKT, and p-AKT.

(D) Quantification of IHC staining intensity in liver tissues for p38, p-p38, AKT, and p-AKT.

(F) Quantification of IHC staining intensity in kidney tissues for p38, p-p38, AKT, and p-AKT. Data are shown as mean ± SD. *P < 0.05, **P < 0.01, ***P < 0.005 by t-test.

(G) Representative H&E staining of kidney and spleen tissues from the indicated treatment groups to assess histopathological alterations. Scale bar = 30 μm.

(H) Western blot analysis of total and phosphorylated p38 and AKT levels in spleen tissues from the indicated groups. GAPDH was used as a loading control.

Discussion

Acute myeloid leukemia (AML) is initiated by driver mutations within hematopoietic stem or progenitor cells (HSPCs), leading to the emergence of leukemia stem cells (LSCs) characterized by extensive self-

renewal capacity and restricted differentiation potential, resulting in the accumulation of immature myeloid cells[18]. Effective and durable anti-leukemic therapies require inducing the death or terminal differentiation of LSCs, which drive disease initiation and relapse[19]. However, achieving this goal has been difficult due to limited understanding of the molecular pathways supporting the self-renewal programs of human AML-LSCs[20]. The selective Bcl-2 inhibitor Venetoclax has demonstrated efficacy as monotherapy in relapsed/refractory (R/R) AML and as part of lower-intensity combined regimens for treatment-naïve elderly AML patients[21]. Venetoclax-based combination therapies for R/R AML have not yet been reported.

In our study, we found that Anlotinib acts as an effective enhancer of Venetoclax in AML, significantly promoting Venetoclax-induced apoptosis. The efficacy and tolerability of Anlotinib combined with chemotherapy in treating solid tumors have been demonstrated[22]. We observed that the combination of Anlotinib and Venetoclax induced substantial growth arrest and apoptosis in AML-LSC lines and patient samples. Current *in vitro* studies and xenograft experiments suggest that Anlotinib–Venetoclax alone may be insufficient for long-term eradication of leukemia stem cells[23, 24]. Importantly, compared with non-leukemic stem cells, our data indicate that sustained exposure to the Anlotinib–Venetoclax combination can control or eradicate LSCs, effectively reducing growth and survival of AML-LSCs cell lines and primary AML-LSCs *in vitro* and *in vivo*. Treating resistant LSCs remains a major obstacle in AML therapy[25]. Interestingly, we demonstrate that SOS1 expression is higher in $CD34^+$ AML-LSC lines than in more differentiated AML cells. Targeting the VEGFR2/SOS1/p38 signaling pathway with TKIs combined with a Bcl-2 inhibitor provides a promising approach to treating LSCs.

In summary, we identified that the combination of Anlotinib and Venetoclax more efficiently kills $CD34^+$ AML-LSCs. This combination demonstrates significant synergistic effects in AML-LSC lines and patient samples compared with non-stem AML. Mechanistically, Anlotinib and Venetoclax together inhibit the VEGFR2/SOS1/p38 signaling pathway, thereby suppressing Mcl-1–mediated Venetoclax resistance. Furthermore, our study reveals the marked efficacy of the combination in a PDX model, providing important preclinical evidence for future clinical application. While our findings support the rationale for expanding Venetoclax-based combinations, clinical evaluation remains essential to determine the efficacy and safety of this therapeutic strategy in patients with AML.

Limitations

This study has some limitations. First, the findings are based primarily on preclinical models, including AML cell lines, patient-derived samples, and xenograft models, which may not fully capture the complexity of the human disease. Second, while the data provide strong mechanistic evidence for the synergistic effects of Anlotinib–Venetoclax, the lack of prospective clinical validation limits the generalizability of the results. Finally, long-term efficacy and potential resistance mechanisms could not be fully addressed within the scope of this study. Future clinical studies are necessary to confirm the safety, tolerability, and therapeutic potential of this combination in patients with AML.

Conclusions

This study provides preclinical evidence that the combination of Anlotinib and Venetoclax effectively targets AML leukemia stem cells by overcoming MCL-1–mediated resistance. Through dual inhibition of survival signaling pathways, this therapeutic strategy enhances apoptosis and prolongs survival in xenograft models. These findings highlight the potential of Anlotinib–Venetoclax as a promising approach to improve treatment outcomes in AML and support future clinical evaluation of this combination.

Abbreviations

AML
Acute myeloid leukemia
AML-LSCs
Acute myeloid leukemia stem cells
BCL-2
B-cell lymphoma 2
MCL-1
Myeloid cell leukemia 1
VEGFR2
Vascular endothelial growth factor receptor 2
PI3K
Phosphoinositide 3-kinase
AKT
Protein kinase B
SOS1
Son of sevenless homolog 1
PDX
Patient-derived xenograft
R/R AML
Relapsed/refractory acute myeloid leukemia
TKI
Tyrosine kinase inhibitor
HSPCs
Hematopoietic stem or progenitor cells

Declarations

Ethics approval

This study was performed in line with the principles of the Declaration of Helsinki. Approval was granted by the First Affiliated Hospital of Xiamen University Ethics Review Board. Informed consent was obtained from the patients before the collection of Bone Marrow samples.

Consent for publication

All contributors have agreed to publish this manuscript.

Competing Interests

There is no conflicting interest to declare.

AI Contribution

During the preparation of this work the authors used ChatGPT (OpenAI) to improve English grammar and readability. After using ChatGPT (OpenAI), the authors reviewed and edited the content as needed and take full responsibility for the content of the publication.

Funding

This work was financially supported by the National Natural Science Foundation of China (82400196 granted for Qian Lai; 82470187 granted for Jie Zha; U22A2090, 82170180 and 81770126 granted for Bing Xu) and the Natural Science Foundation of Fujian Province (2023J06054 granted for Jie Zha). Xiamen Municipal Bureau of Science and Technology (3502Z20234001 granted for Jie Zha).

Author Contributions

Conceptualization, J. Zha, B. Xu, Q. Lai; Methodology, B.W. Hou ; Y.C. Li, J.W. Yao; Software, Y.C. Li; Validation, Y.L. Jiang, J. Zha, B. Xu; Formal Analysis, Y.L. Jiang; Resources, B. Xu; Data Curation, J. Zha, B. Xu; Writing - Original Draft Preparation, Y.L. Jiang, B.W. Hou, Q. Lai; Supervision, J. Zha, B. Xu, Q. Lai; Funding Acquisition, J. Zha, B. Xu, Q. Lai; All authors have read and approved the final manuscript.

Acknowledgements

Not applicable.

Data Availability

The datasets generated during the current study are available from the corresponding author on reasonable request.

References

1. Kantarjian HM, DiNardo CD, Kadia TM, Daver NG, Altman JK, Stein EM, et al. Acute myeloid leukemia management and research in 2025. CA Cancer J Clin. 2025;75(1):46–67.

2. Dohner H, Wei AH, Appelbaum FR, Craddock C, DiNardo CD, Dombret H, et al. Diagnosis and management of AML in adults: 2022 recommendations from an international expert panel on behalf of the ELN. Blood. 2022;140(12):1345–77.
3. Bhansali RS, Pratz KW, Lai C. Recent advances in targeted therapies in acute myeloid leukemia. J Hematol Oncol. 2023;16(1):29.
4. Stelmach P, Trumpp A. Leukemic stem cells and therapy resistance in acute myeloid leukemia. Haematologica. 2023;108(2):353–66.
5. Yao Y, Li F, Huang J, Jin J, Wang H. Leukemia stem cell-bone marrow microenvironment interplay in acute myeloid leukemia development. Exp Hematol Oncol. 2021;10(1):39.
6. Melgar K, Walker MM, Jones LM, Bolanos LC, Hueneman K, Wunderlich M, et al. Overcoming adaptive therapy resistance in AML by targeting immune response pathways. Sci Transl Med. 2019;11(508):[Check eLocator].
7. Jones DL, Wagers AJ. No place like home: anatomy and function of the stem cell niche. Nat Rev Mol Cell Biol. 2008;9(1):11–21.
8. Waclawiczek A, Leppa AM, Renders S, Stumpf K, Reyneri C, Betz B, et al. Combinatorial Bcl-2 family expression in acute myeloid leukemia stem cells predicts clinical response to azacitidine/venetoclax. Cancer Discov. 2023;13(6):1408–27.
9. DiNardo CD, Pratz K, Pullarkat V, Jonas BA, Arellano M, Becker PS, et al. Venetoclax combined with decitabine or azacitidine in treatment-naive, elderly patients with acute myeloid leukemia. Blood. 2019;133(1):7–17.
10. Wang D, He J, Liu S, Zhang H, Tang D, Chen P, et al. Anlotinib synergizes with venetoclax to induce mitotic catastrophe in acute myeloid leukemia. Cancer Lett. 2024;593:216970.
11. Kasper S, Breitenbuecher F, Heidel F, Hoffarth S, Markova B, Schuler M, et al. Targeting Mcl-1 sensitizes FLT3-ITD-positive leukemias to cytotoxic therapies. Blood Cancer J. 2012;2(3):e60.
12. Bhatt S, Pioso MS, Olesinski EA, Yilma B, Ryan JA, Mashaka T, et al. Reduced mitochondrial apoptotic priming drives resistance to BH3 mimetics in acute myeloid leukemia. Cancer Cell. 2020;38(6):872 – 90.e6.
13. Carter JL, Su Y, Al-Antary ET, Zhao J, Qiao X, Wang G, et al. ONC213: a novel strategy to resensitize resistant AML cells to venetoclax through induction of mitochondrial stress. J Exp Clin Cancer Res. 2025;44(1):10.
14. Zhou M, Chen X, Zhang H, Xia L, Tong X, Zou L, et al. China National Medical Products Administration approval summary: Anlotinib for the treatment of advanced non-small cell lung cancer after two lines of chemotherapy. Cancer Commun (Lond). 2019;39(1):36.
15. Li H, Feng H, Zhang T, Wu J, Shen X, Xu S, et al. CircHAS2 activates CCNE2 to promote cell proliferation and sensitizes the response of colorectal cancer to anlotinib. Mol Cancer. 2024;23(1):59.
16. Rahmani M, Nkwocha J, Hawkins E, Pei X, Parker RE, Kmieciak M, et al. Cotargeting Bcl-2 and PI3K induces BAX-dependent mitochondrial apoptosis in AML cells. Cancer Res. 2018;78(11):3075–86.

17. Zhou H, Qin D, Xie C, Zhou J, Jia S, Zhou Z, et al. Combinations of HDAC inhibitor and PPAR agonist induce ferroptosis of leukemic stem cell-like cells in acute myeloid leukemia. Clin Cancer Res. 2024;30(23):5430–44.
18. Cain TL, Derecka M, McKinney-Freeman S. The role of the haematopoietic stem cell niche in development and ageing. Nat Rev Mol Cell Biol. 2025;26(1):32–50.
19. Li Z, Ma R, Ma S, Tian L, Lu T, Zhang J, et al. ILC1s control leukemia stem cell fate and limit development of AML. Nat Immunol. 2022;23(5):718–30.
20. Chung SS, Hu W, Park CY. The role of microRNAs in hematopoietic stem cell and leukemic stem cell function. Ther Adv Hematol. 2011;2(5):317–34.
21. Konopleva M, Pollyea DA, Potluri J, Chyla B, Hogdal L, Busman T, et al. Efficacy and biological correlates of response in a phase II study of venetoclax monotherapy in patients with acute myelogenous leukemia. Cancer Discov. 2016;6(10):1106–17.
22. Cheng Y, Chen J, Zhang W, Xie C, Hu Q, Zhou N, et al. Benmelstobart, anlotinib and chemotherapy in extensive-stage small-cell lung cancer: a randomized phase 3 trial. Nat Med. 2024;30(10):2967–76.
23. Jiang Y, Liu L, Jiang Y, Li Z, Feng L, Zhuang X, et al. Preclinical evaluation of the multiple tyrosine kinase inhibitor anlotinib in leukemia stem cells. Pharmaceuticals (Basel). 2022;15(11):[Article ID needed].
24. Short NJ, Daver N, DiNardo CD, Kadia T, Nasr LF, Macaron W, et al. Azacitidine, venetoclax, and gilteritinib in newly diagnosed and relapsed or refractory FLT3-mutated AML. J Clin Oncol. 2024;42(13):1499–508.
25. Paczulla AM, Rothfelder K, Raffel S, Konantz M, Steinbacher J, Wang H, et al. Absence of NKG2D ligands defines leukaemia stem cells and mediates their immune evasion. Nature. 2019;572(7768):254–9.
26. Supplemental Information

Tables

Table 1 is available in the Supplementary Files section.

Figures

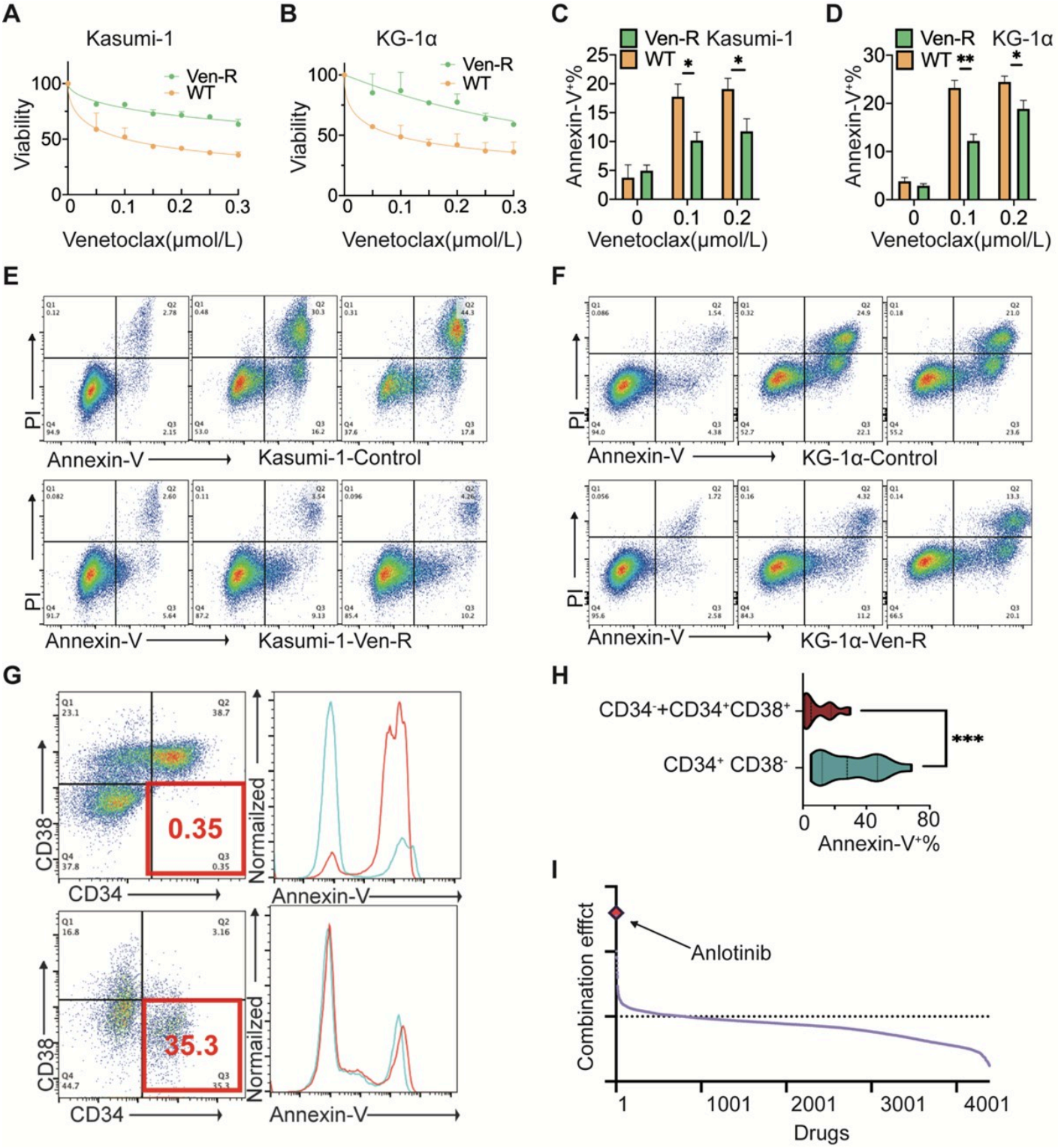


Figure 1

Anlotinib is the potential combination choice for Venetoclax-resistant LSC

(A, B) Cell viabilities in Venetoclax-resistant Kasumi-1-R and KG-1α-R cells for 24 hours.

(C, D) Quantification of apoptosis in leukemia stem-like cell lines Kasumi-1 wild type and Kasumi-1 Venetoclax-resistant cell lines after treatment with Venetoclax for 24 h.

(E, F) Flow cytometry plots depict the gating approach used to identify apoptotic cells in Kasumi-1 wild-type and Kasumi-1 Venetoclax-resistant cell lines by staining Annexin V(AV) and Propidium iodide(PI).

(G)Flow cytometry plots depict the gating approach used to identify the primary leukemia stem cell by stanning human CD34 and human CD38 and the apoptotic cells by stanning Annexin V(AV).

(H)Quantification of apoptosis in primary leukemia stem cell after treatment by Venetoclax for 24 h.

(I)High-throughput drug screening identifies Anlotinib as a synergistic compound with Venetoclax in targeting leukemia stem-like cells.

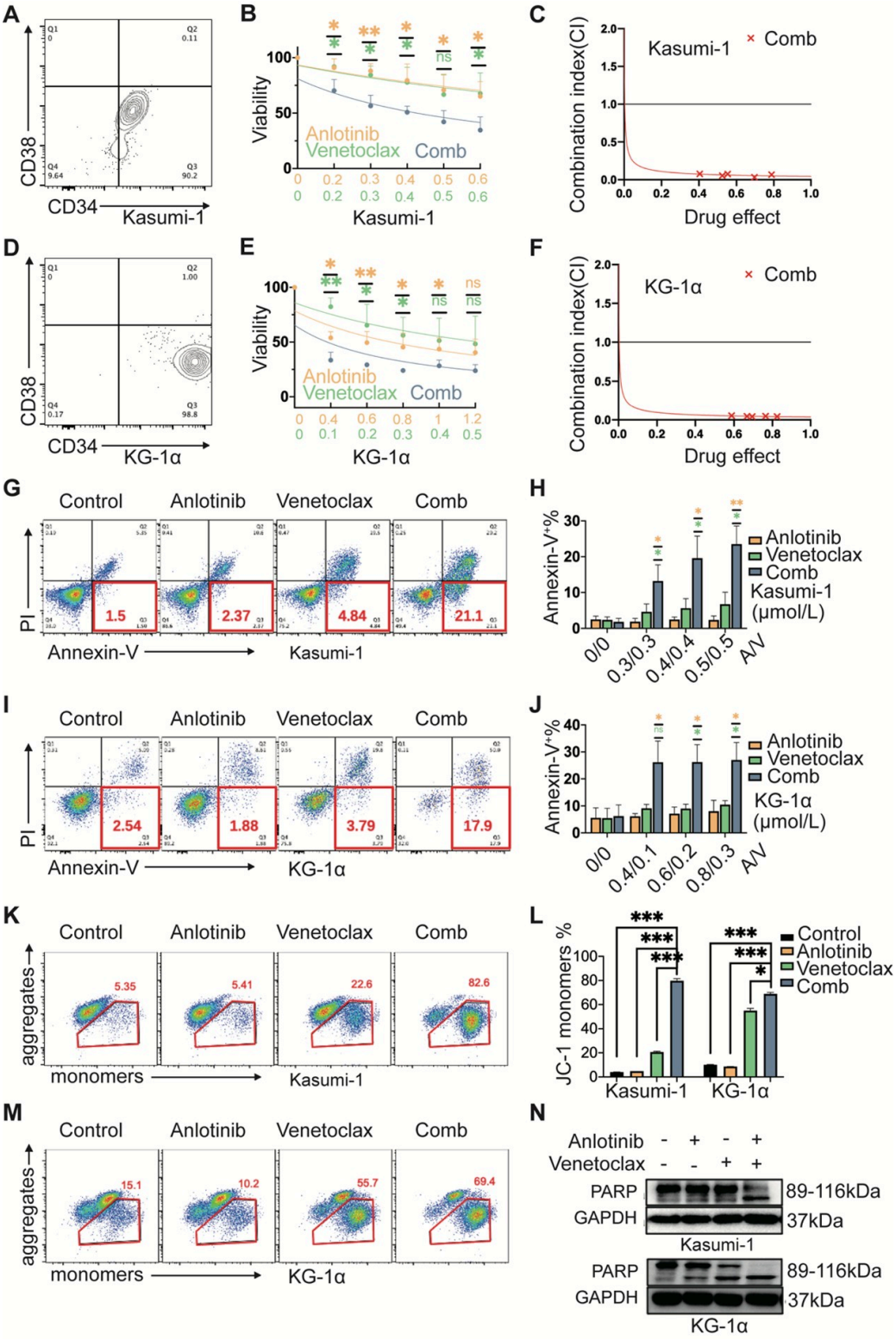


Figure 2

Anlotinib resensitize the Venetoclax-resistant LSC cell through increasing cell apoptosis.

(A, D) Immunomarker of leukemia stem-like cells in Kasumi-1 and KG-1α cell lines by flow cytometry.

(B, E) Proliferation analysis of leukemia stem-like cell lines Kasumi-1 and KG-1α after treatment with combined candidate drugs and Venetoclax.

(C,F) Combination index (CI) in the indicated two cell line cells was analyzed by CalcuSyn software. CI > 1 indicates antagonist effect; CI = 1 indicates additive effect; CI < 1 indicates synergistic effect.

(G,I) Flow cytometry plots depict the gating approach used to identify apoptotic cells in Kasumi-1 and KG-1α cell lines by staining AV and PI.

(H,J) Quantification of apoptosis in leukemia stem-like cell lines Kasumi-1 and KG-1α. Bar graphs show the percentage of Annexin V-positive, PI-negative early apoptotic cells in Kasumi-1 and KG-1α cell lines, as determined by flow cytometry.

(K,M) Gating strategy for mitochondrial membrane potential analysis in leukemia stem-like cell lines Kasumi-1 and KG-1α using JC-1 staining.

(L) Quantification of mitochondrial membrane potential changes in leukemia stem-like cell lines Kasumi-1 and KG-1α using JC-1 staining.

(N) Western blot analysis of the apoptosis marker PARP in leukemia stem-like cell lines Kasumi-1 and KG-1α under different drug treatment for 12 hours.

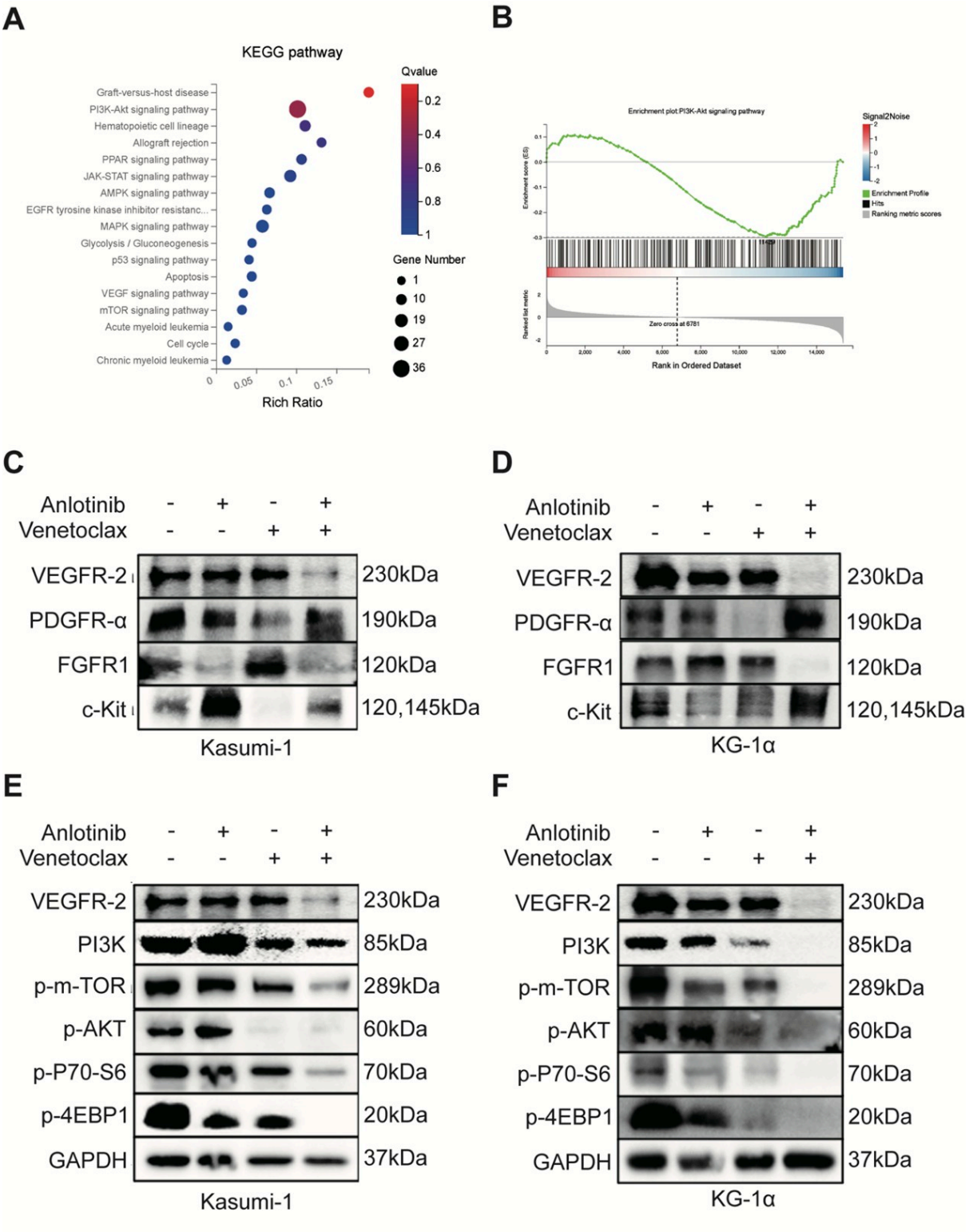


Figure 3

Anlotinib enhance the effect of Venetoclax in inhibiting the VEGF/PI3K/AKT signaling pathway

(A) KEGG enrichment analysis of differential expression genes detected by RNA-Seq of Kasumi-1 cell line comparing combination regimen and venetoclax-only regimen.

(B) GSEA enrichment analysis of differential expression genes detected by RNA-Seq of Kasumi-1 cell line comparing combination regimen and venetoclax-only regimen.

(C,D) The expression levels of the targets protein of Anlotinib in Kasumi-1,KG-1α cell lines.

(E,F)Expression and phosphorylation levels of PI3K/AKT signaling pathway in Kasumi-1, KG-1α cell lines after the treatment of combining Anlotinib and Venetoclax and alone.

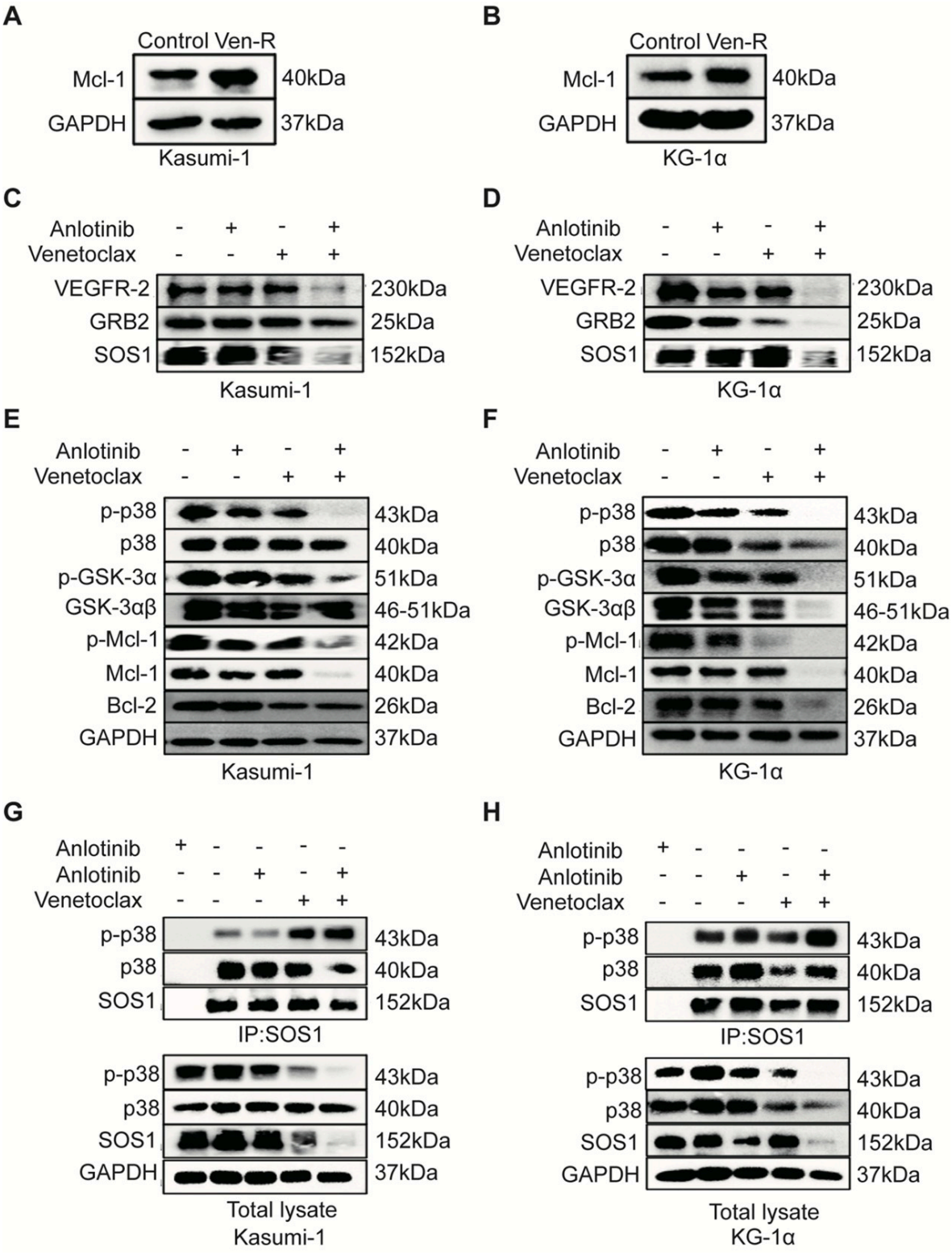


Figure 4

Anlotinib reverses Venetoclax-induced overexpression of Mcl-1 by inhibiting SOS1.

(A,B) Western blot shows the original expression of Mcl-1 and Bcl-2 in Venetoclax-resistant Kasumi-1-R and KG-1α-R cells.

(C,D) Immunoblots showing the levels of indicated protein in Kasumi-1 and KG-1α cells after treatment with Anlotinib and Venetoclax alone and combination.

(E,F) The expression of p38/GSK3/ Mcl-1 pathway signaling in Kasumi-1 and KG-1α cells.

(G,H) SOS1 can accumulate p-p38 in response to the treatment of combination of the Anlotinib and Venetoclax.

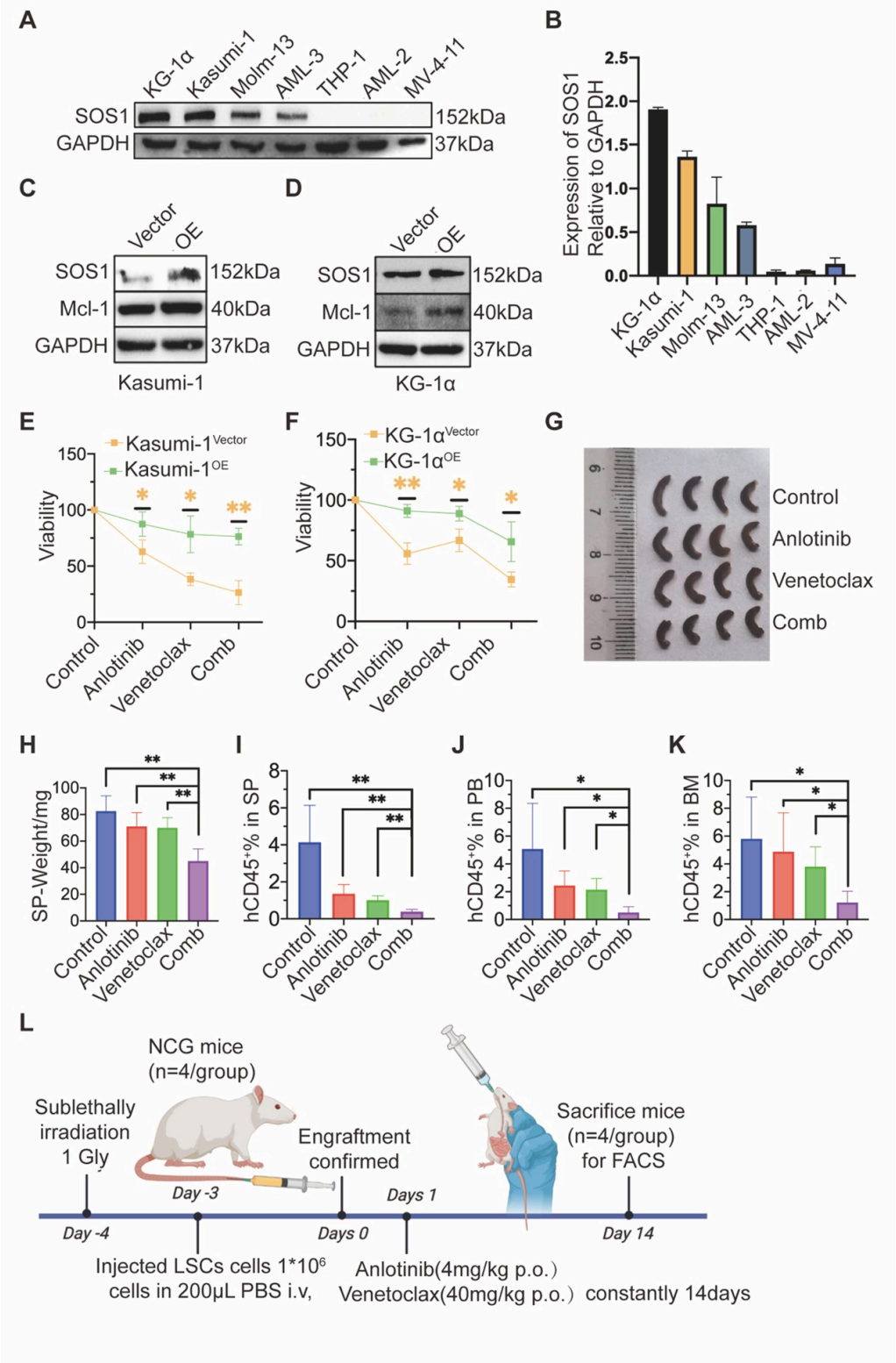


Figure 5

SOS1 activation restores Venetoclax resistance in LSCs *in vitro*.

(A,B) Basic expression of SOS1 in KG-1α, Kasumi-1, MOLM-13, OCI-AML-2, OCI-AML-3,THP-1, and MV-4 11 cells.

(C,D) Immunoblotting of SOS1 and Mcl-1 in SOS1 overexpressed and wild type AML-LSCs cell lines.

(E,F) Cell viability test of the SOS1 overexpressed and wild type AML-LSCs cell lines.

(G) Representative spleen images of CDX models of gavage carrier, Alotinib, Venetoclax, or their combination.

(H) Quantitative analysis of spleen weight (n=4/group).

(I-K) Flow cytometry revealed the percentage of $hCD45^{+}$ leukemic cell proportion in spleen, peripheral blood and bone marrow for Kasumi CDX models.

(L) Schematic outline of the CDX model.

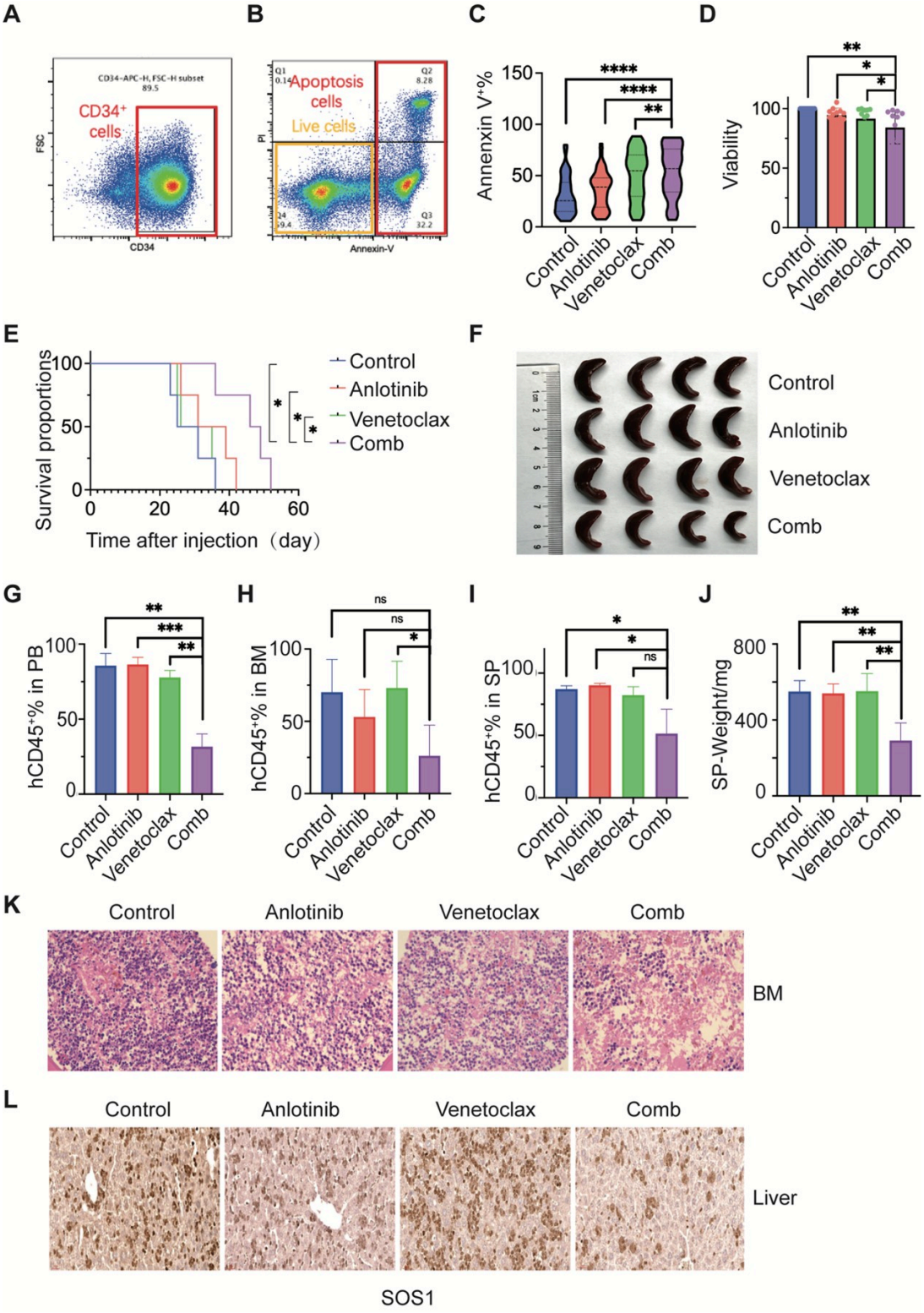


Figure 6

The combination of Anlotinib and Venetoclax reciprocally overcome the resistance of AML primary samples *in vitro* and *in vivo*.

(A,B) Flow cytometry showing the gate strategy to determine $CD34^+$ AML LSC subpopulation.

(C) Apoptosis rates of $CD34^+$ primary AML sample induced by the combination of Anlotinib and Venetoclax for 12 hours.

(D) Cell viability test of $CD34^+$ primary AML sample upon the combination of Anlotinib and Venetoclax for 12 hours.

(E) The survival was monitored over time and the Kaplan-Meier survival curves of PDX (n=4/group) was shown. Statistical significance was evaluated the long rank test.

(F) Representative spleen images of PDX models of gavage carrier, Anlotinib, Venetoclax, or their combination.

(G-I) Flow cytometry analysis of hCD45 percentage in peripheral blood,bone marrow and spleen was shown.

(J)The spleen weight of mice in the four groups was assessed at the same time points after sacrificed.

(K) Representative HE staining of PDX mice bone marrow.

(L) Representative IHC staining of SOS1 in PDX mice liver.

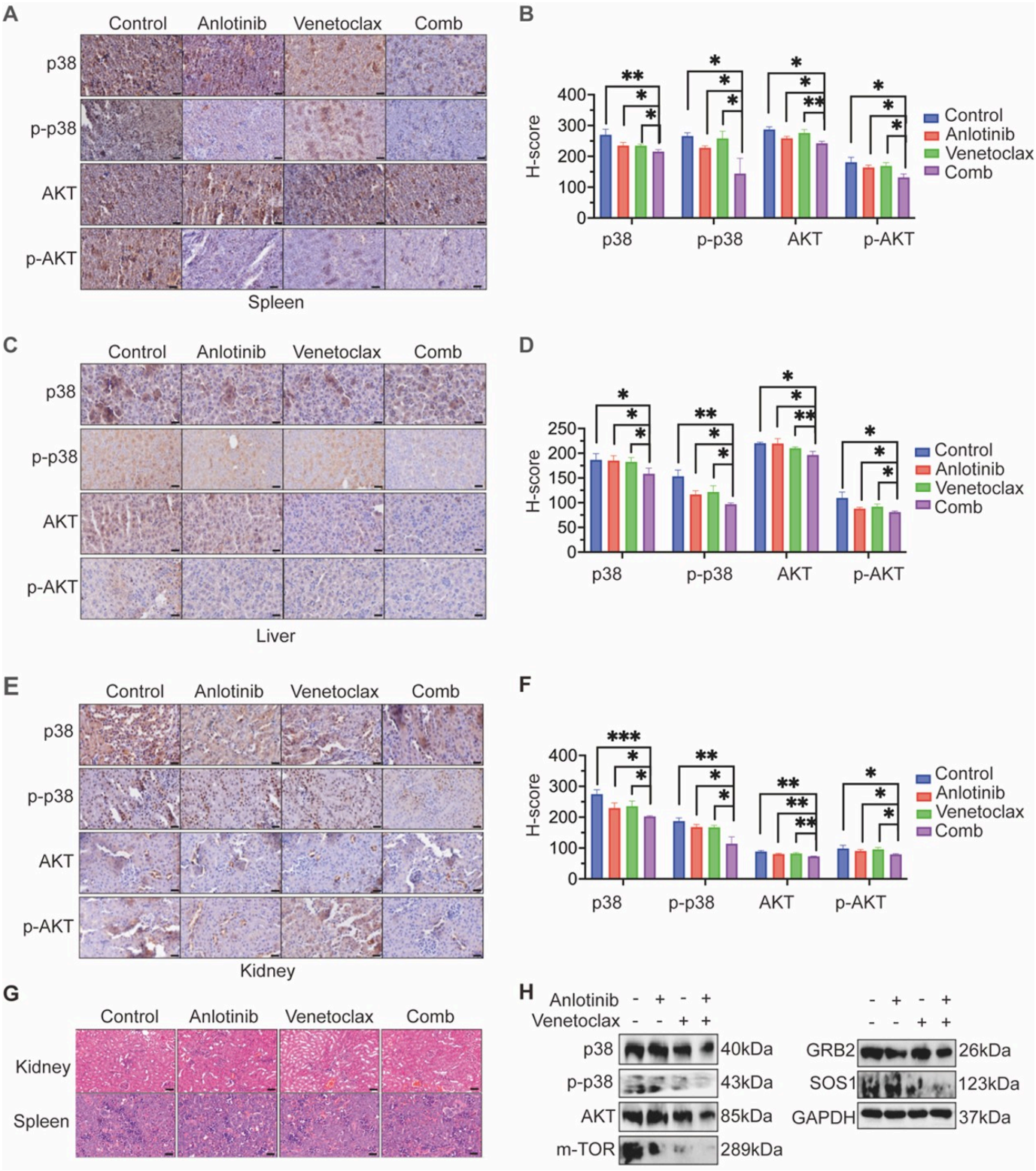


Figure 7

Inhibition of p38 and AKT signaling by combination treatment in PDX models.

(A, C, E) Representative IHC staining images of spleen (A), liver (F), and kidney (K) tissues from PDX mice treated with vehicle (Control), Anlotinib, Venetoclax, or the combination (Comb). Sections were

stained for total p38, phosphorylated p38 (p-p38), total AKT, and phosphorylated AKT (p-AKT). Scale bar = 30 μm.

(B) Quantification of IHC staining intensity in spleen tissues for p38, p-p38 AKT, and p-AKT.

(D) Quantification of IHC staining intensity in liver tissues for p38, p-p38, AKT, and p-AKT.

(F) Quantification of IHC staining intensity in kidney tissues for p38, p-p38, AKT, and p-AKT. Data are shown as mean ± SD. *P < 0.05, **P < 0.01, ***P < 0.005 by t-test.

(G) Representative H&E staining of kidney and spleen tissues from the indicated treatment groups to assess histopathological alterations. Scale bar = 30 μm.

(H) Western blot analysis of total and phosphorylated p38 and AKT levels in spleen tissues from the indicated groups. GAPDH was used as a loading control.

Supplementary Files

This is a list of supplementary files associated with this preprint. Click to download.

- floatimage11.png
- Onlinefloatimage10.png
- Onlinefloatimage9.png